Pew^2: Open-source imaging software for laser-ablation inductively-coupled-plasma mass-spectrometry.

Thomas E. Lockwood, Mika T. Westerhausen, Philip A. Doble*.

The Atomic Medicine Initiative, University of Technology Sydney, Ultimo, New South Wales, Australia.

ABSTRACT: Open-sourced software is a key component of the mass-spectrometry imaging field, where transparency in data processing is vital. Imaging of trace elements and immunohistochemically labelled biomolecules in tissue sections is typically performed using laser ablation inductively-coupled plasma mass-spectrometry (LA-ICP-MS). However, efficient and facile processing of images is hampered by a lack of verifiable and user-friendly software that supports multiple LA-ICP-MS platforms. In this paper we introduce Pew^2, an LA-ICP-MS specific and feature-rich open-source image processing software that is compatible with common ICP-MS vendors. Pew^2 is designed to be fast, easy to use and adheres to modern visualisation philosophies to maximise productivity and to minimise data interpretation errors and image anomalies.

The high sensitivity of laser-ablation inductively-coupled plasma mass-spectrometry (LA-ICP-MS) makes it the preferred technique for imaging trace elements in biological tissues. Since the seminal paper of Gray[1] there has been significant improvements in the speed, sensitivity and resolution of LA-ICP-MS imaging with growing utility for medical,[2] life science,[3] environmental,[4] geoscience[5] and food safety applications.[6] However, there has been sporadic development of data reduction software with no preferred open-source option available. While a large library of software does exist for the conversion and analysis of MS-imaging (MSI) data,[7] very few of these programs focus on LA-ICP-MS data specifically (Table 1). These are confined to specific vendor file formats,[8] require purchase of an expensive commercial license[9] or are closed-source.[10] This is partially driven by a lack of vendor support for LA-ICP-MS imaging.

Table 1. Published software for LA-ICP-MS data processing. Most software no longer available and has poor vendor support.

Program	Import Formats	Availability
ELAI VBA script[11]	Pre-formatted	Unavailable
HDIP[9]	Multiple	Commercial
IMAGENA[12]	Pre-formatted	Unavailable
iQuant2[10]	Pre-formatted	Unavailable
LA-ICP-MS Image Tool[13]	Pre-formatted	Open-source
LA-iMageS[8]	PerkinElmer	Open-source
Iolite 4[14]	Multiple	Commercial
Iolite 2 (add ref)	Multiple	Freeware
MapIT! MATLAB script[15]	Pre-formatted	Open-source
RecSegImage-LA[16]	Pre-formatted	Open-source

Initially LA-ICP-MS data was collected in a spot-wise manner, similar to other MSI techniques, where images were constructed via integration of signal peaks produced by ablation of a grid of individual spots.[17] In contrast, most LA-ICP-MS methods today use continuous collection of individual lines. The laser is usually configured to continuously ablate a line such that each MS acquisition window forms a single pixel of an image. Typically, the laser scan speed, spot diameter and MS acquisition time are set for equal aspect pixels.[18] The separate spots or lines must then be combined to form a complete image. Quantitative imaging is possible by simultaneously or consecutively sampling material of a known concentration. A calibration curve is constructed by plotting signal intensities against concentrations and samples quantified by comparison to a line of best fit. This combination of spatially resolved and quantified elemental imaging provides in depth analysis of biological systems normally only possible by multiple techniques.

Each ICP-MS vendor and instrument stores and exports data in different formats, usually with little consideration for imaging applications. Consequently, vendor exports require pre-processing prior to examination of data using external imaging software.[8] Time spent manually pre-processing data files is often longer than analysis time, a problem that increases exponentially with data size and is further multiplied when each instrument requires a separate process. Most available software does little to assist users in importing data, mainly due to the complexities to support a large variety of file formats. Only closed-source commercial product software platforms natively supports more than one vendor format.[9,14]

Open sourcing software provides many benefits and enables users to collaborate and build upon existing software. In the field of bioimaging one such example is FIJI, an image processing package based on ImageJ. FIJI has a fully open development stream and ubiquitous usage in literature.[19] Public visibility of code allows users to verify implemented algorithms that ensures confidence in performance and outputs. This code

visibility allows users to contribute features such as support for new vendors and instruments. Open sourcing also provides opportunities for other developers to maintain the software if the original designer abandons the project. This is seen extensively with published LA-ICP-MS software where many programs fail to receive meaningful updates a year after publication and lack support for newly released instruments or formats.

The usual scientific publication model relies on peer review to ensure quality, robust interpretation, and appropriate reporting of results and conclusions. However, this is not true of unreviewable closed commercial software. Open-source software usage is the future of research with large entities such as CERN moving to a totally open-source framework in order to improve collaborative efficiency.[20] This model would be particularly valuable for the growing field of LA-ICP-MS imaging, which is finding ever increasing applications in many diverse areas of endeavour.

User experience and documentation of features contribute to software's ease of use and facilitates widespread adoption. This is true for software in all fields and is an educational pillar for computer science and software engineering courses.[21] Documentation accelerates acceptance of new features and techniques as software development progresses with research. Documentation is not common in LA-ICP-MS imaging software, inhibiting widespread implementation, and preventing use of full feature sets. Current LA-ICP-MS programs also fail to adhere to unbiased visualisation philosophies, potentially leading to misidentification and obfuscation of data.[22] Despite a large amount of research into visualisation methods, the majority of published ICP-MS imaging software default to misleading rainbow colour-maps.[23] The non-uniformity in perceptual contrast of these colour-maps can introduce apparent artifacts and lead to incorrect interpretations.[24] These issues can be completely negated by using a perceptually uniform colour-map.

Image processing is often used to improve the clarity of experimental data to better communicate results. Displaying regions of interest (ROIs), signal overlaps and the removal of instrumental anomalies all simplify the interpretation of data. Segmentation[25] and ratiometric analysis[26] of LA-ICP-MS images have been used to identify structural features and filters such as numerical inversion of blur[27] and Richardson-Lucy deconvolution[28] have been used to remove system artefacts. These tools are quickly becoming essential for LA-ICP-MS imaging applications.

We developed a novel LA-ICP-MS imaging program, Pew², to address the shortcomings of current software and to simplify the import and conversion of spot-wise and line-by-line acquired quantitative data. This new software is an open-source, python-based implementation using 'NumPy',[29] with a cross-platform Qt5 graphical user interface (GUI) implemented using 'PySide2'. A python library 'pewlib' has been made available for creation of python scripts for batch conversion of data and processing. Drag-and-drop import of Agilent, PerkinElmer and Thermo instrument data removes any need for pre-processing, greatly reducing user workload. Support for other vendors is maintained with a flexible text-image (2D delimited text files) and file-per-line importer.

EXPERIMENTAL
LA-ICP-MS Analysis

To demonstrate the use of Pew² a 1.5 mm human pancreatic adenocarcinoma tissue micro-array core (US Biomax; Rockville, MD) was imaged using a NWR193 laser ablation system (Kenelec Scientific; Frenchs Forest, Australia) coupled to an Agilent Technologies 8900 ICP-MS (Mulgrave, Australia). The laser was operated at 40 Hz with a 10 μm beam diameter and scan speed of 40 μm s^{-1}. Laser fluence was 0.4 J cm^{-2}. A total acquisition time of 0.25 s was used to produce square image pixels. Quantification of the tissue was performed using gelatine calibration standards prepared as per Westerhausen et al.[30]

Software Design

Pew² was written in python using the 'NumPy' and 'PySide2' libraries and is available on github (https://github.com/djdt/pewpew). NumPy is a powerful array programming library that efficiently accesses and computes multidimensional data.[29] Image processing operations in Pew² take advantage of NumPy's vectorisation to ensure performant code. A modern, cross-platform Qt5 based GUI was implemented using PySide2, the official python bindings for Qt. The wide availability of both these libraries means that Pew² can be compiled on modern operating systems, maximising its availability. A python library 'pewlib' (https://github.com/djdt/pewlib) that implements the import and export of data as well as basic data processing, is also available. This library can be used to easily load data for use into python scripts, allowing further processing and batch operations.

RESULTS AND DISCUSSION
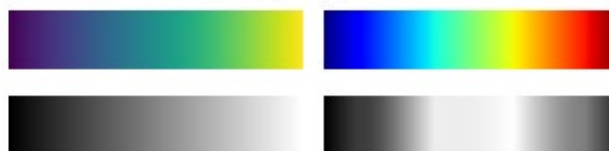### Visualisation

Figure 1. Comparison of colour-maps Viridis (left) and Jet (right) and their Lab colour lightness channels (bottom row). The sharp changes in contrast of Jet can introduce perceptual artefacts when interpreting images.

The primary focus of any LA-ICP-MS imaging program is the visualisation of data. Trends and features in images are determined from false-colour representations of MS signals and the interpretation of this colouring should therefore be clear.[23] Commonly used rainbow colour maps have non-uniform colour gradients and low contrast features that occupy a small region of the colour-map increasing the possibility of misinterpretation due to sharp transitions in contrast and improper grouping, apparent in Figure 1. Pew² implements a range of colour-maps where the change in perceived colour is uniform across the entire map. These colour maps alleviate any risk of misinterpretation allowing for transparent depictions of MS signals.

Data Import

Pew² is suitable for direct import of a variety of vendor formats of both sample and calibration data according to the workflow shown in Figure 2, avoiding the need for data pre-processing for the most common instruments. Drag-and-drop importation of raw Agilent batches (MassHunter G7200B or later), PerkinElmer Elan 'XL', Thermo Fischer Qtegra exports, as well as both text-image and file-per-line exports for easy loading of

data. Importing files also reads any available instrument parameters such as the MS acquisition time and applies them to the image configuration. Non-natively supported instruments can still be imported, however they require preformatting prior to import.
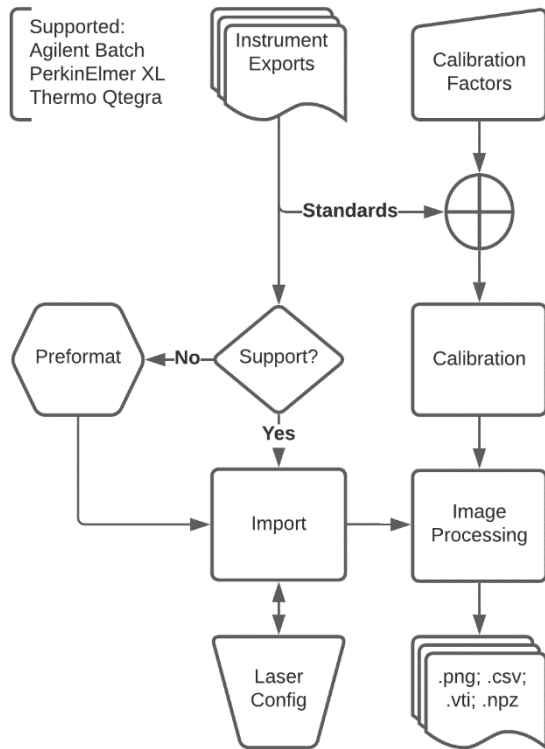

Figure 2. Typical workflows for import and analysis of LA-ICP-MS data using Pew².

While the primary focus of Pew² is line-by-line collected data, importation of spot-wise data is also implemented. A variety of peak detection techniques such as simple or windowed thresholding and continuous wavelet transforms (Figure 3) have been incorporate for accurate peak detection even in situations where background signal is not uniform.[31] A single 'marker' element is used to guide the integration of peaks and an image for each element is constructed using the peak height or area. However, this requires at least one element to be present across the entirety of the sample and for the positions of peaks for each element to be similar.
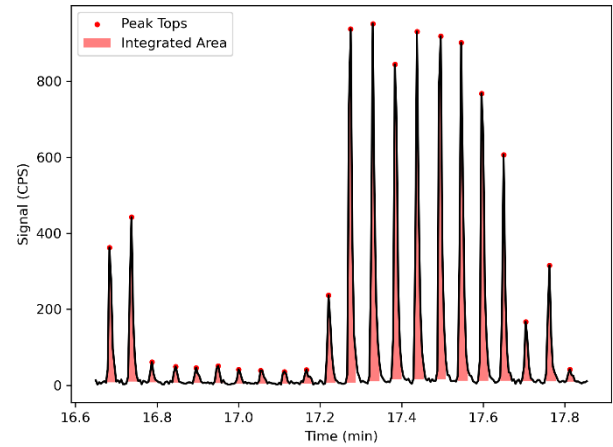

Figure 3. Integration of peaks following detection using continuous wavelet transformation. The red area of each peak may be used to produce pixels in the LA-ICP-MS image.

As Agilent MassHunter is directly supported by Pew² the data for both the sample and standard may be imported by drag-and-drop of the batch folders into the main window. Data is read directly from the MassHunter binary files created on collection of each line. The correct acquisition time is automatically applied to the image using average difference of recorded acquisition event times (to the nearest µm). Following import, the laser spot-size and speed are entered manually to ensure the correct image aspect and correct sizing of the scale-bar (Figure 4). The calibration standards may be imported in a similar fashion before being loaded into the built-in standardisation tool.
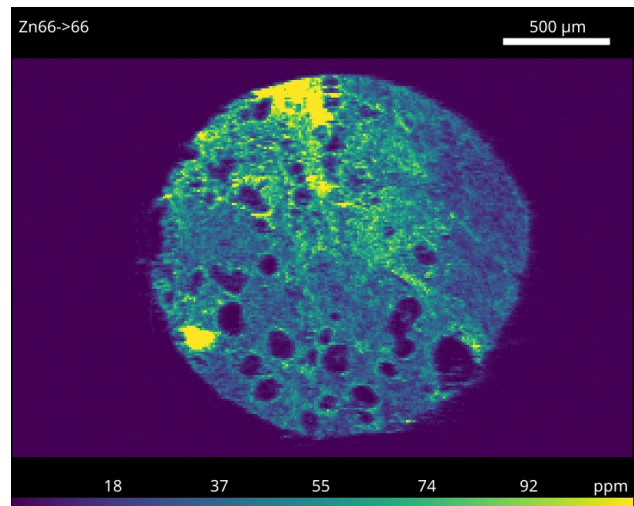

Figure 4. Image of ^{66}Zn imported into Pew². The scale and colour bars depict accurate input of laser and calibration parameters.

Calibration

Like most MS based techniques, LA-ICP-MS data uses calibration factors for quantification. These factors are collected by ablating materials of known concentrations before, after or during the sampling of a specimen. Calibration factors are then calculated from a linear fit of the known concentrations to MS responses. Pew² allows direct input of externally calculated factors and provides an area-based standardisation tool, where the

user can assign rectangular areas of an image to specific calibration values (Figure S1). Values are then used to calculate a line of best fit and relevant coefficients for assessing validity (Table 2). Weighting of the linear regression may also be used to increase accuracy in the lower end of the calibration range as signal deviations are typically non-uniform across a calibrated range.[32] These calibrations can then be saved and applied to other open images or exported for external use.

Table 2. Calibration coefficients calculated by the software.

Element	Intercept	Gradient	r^2	$S_{y, x}$
^{55}Mn	7.06	29.20	0.9931	4.7
^{56}Fe	11.41	18.71	0.9959	24.6
^{63}Cu	4.01	2.04	0.9940	0.6
^{66}Zn	8.48	4.12	0.9915	4.5

Data Processing

Image processing is essential for researchers to better communicate their results. Removal of instrument noise and selection of ROIs often clarify and focus an image's meaning for easier interpretation by readers. Drift correction, filtering and calculator tools built into Pew² enable removal of instrument artefacts and improved image interpretability. Changes in laser, plasma or MS conditions may cause signal drift and result in a distorted image. While drift should be minimised by using shorter runs and correctly 'warming up' the instruments, it can be mitigated when quantification is not required. The drift tool calculates a polynomial fit in the direction of acquisition in a user-defined slice of the background, which is then used to renormalise the image (Figures S2 and S3). Spikes in data, and regions of extremely low or high signal resulting from instrument noise may be removed by applying a local (mean or median) filter at the position of each spike. Spikes are identified by comparing pixel values to the mean or median of its surrounding values, if the value is above a user defined threshold, such as 3 times the standard deviation then it is replaced with the local mean or median value (Figure S4). The filtering threshold must be carefully selected to prevent alteration of valid signal. These features correct variation in raw signal, resulting in production of consistent and easily interpretable images.

Segmentation is a fundamental imaging analysis tool used to isolate ROIs from the background. This can be performed either manually or automatically using image thresholding, as in Figure 5. Automatic, or unsupervised, methods have the advantage of removing biases than a user can introduce when manually selecting ROIs. Pew² has multiple image thresholding methods built in including manual selections, binary filters such as median and Otsu's method, as well as multiple level k-means thresholding (Figure 5). Binary filters are typically used to separate signal from the
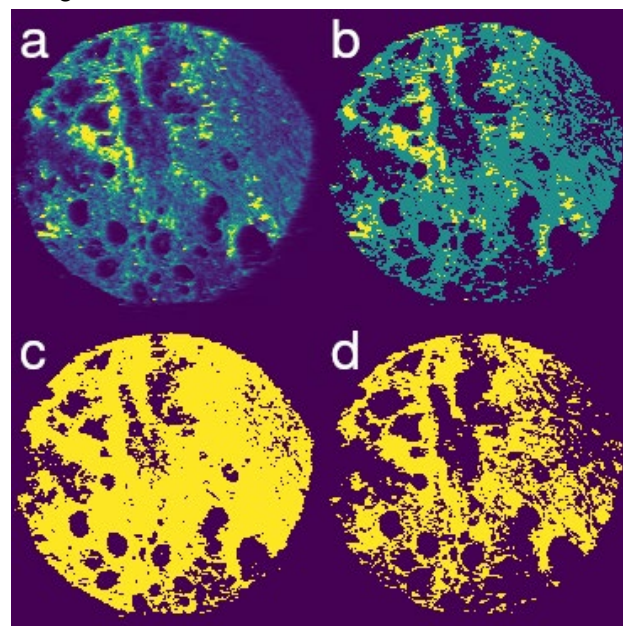

Figure 5. Unsupervised segmentation of ^{56}Fe (a) using three-level k-means (b), mean thresholding (c) and Otsu's method (d). The masks produced by each algorithm can be used for removal of background and image feature selection.

background, while multiple level filters allow specific area quantification in systems where the sample consists of multiple structural features, not all of which should be included in quantified data.[16]

Construction of images as ratios of two or more elements is a useful analysis technique for normalisation and feature contrast.[26] Normalisation allows samples and ROIs where a non-uniform amount of material is ablated, such as those with different thickness, to be compared. Ratiometric analysis has also been used to perform internal standardisation of LA-ICP-MS data and analysis of isotopic ratios. Pew² greatly simplifies the way these types of images can be constructed; given an image with elements A and B a user only is required to enter A / B into the formula to produce an image of the ratio. The calculator also implements several useful functions and can parse if-then-else statements, enabling thresholding of both images and calculations. By combining functions and operations a user can perform isotopic analysis, ratiometric quantification, background removal and other Boolean operations.
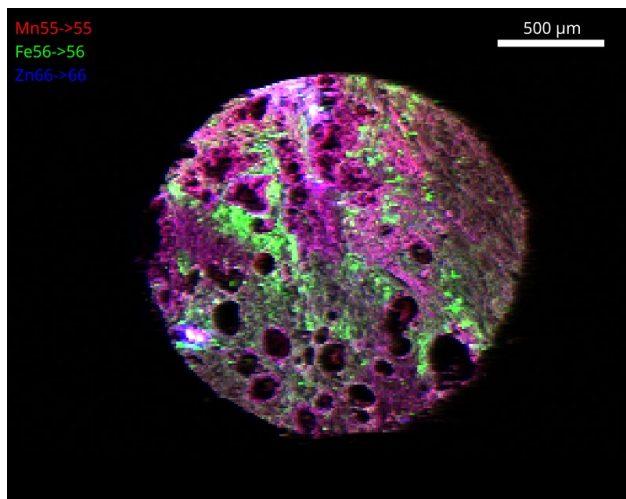
Elemental Overlays

Figure 6. RGB overlay of ^{55}Mn (red), ^{56}Fe (green) and ^{66}Zn (blue). The colocalization of Mn and Zn is clearly visible as magenta regions within the image.

It is often desirable to be able to view multiple elemental images at once, for visual assessment of the spatial relationship of elements. The image overlay tool in Pew^2 allows viewing of up to three elements simultaneously using RGB or CMYK colouring. The spatial overlap of Mn (red) and Zn (blue) and spatial difference of Fe (green) were able to be visualised using this tool (Figure 6). A numerical representation of this overlap was then calculated in Pew^2 using Pearson's R correlation coefficients (Equation 1) using the pixel values of two images. Both the image and the values in Table 3 show a correlative spatial relationship between Mn and Zn. Other colocalisation coefficients may be calculated using the approach developed by Costes et al.[33]

$$ r = \frac{\sum (x_i - \bar{x})(y_i - \bar{y})}{\sigma_x \sigma_y} $$

Table 3. Pearson's R correlation coefficients for the elements measured in the TMA core.

	^{55}Mn	^{56}Fe
^{66}Zn	0.80	0.26
^{56}Fe	0.37	-

Data Export

While Pew^2 has some built in image processing capability, a large selection of field specific image analysis software is already available.[19,34] Image exports in '.csv' (text image), '.png' and '.vti' (VTK ImageData) formats maximise compatibility with these programs. However, these formats fail to store the laser configuration and calibration data of images which leads to unnecessary work in future reanalysis. To address this, a custom export using NumPy archives is used to compactly store the image data, configuration and calibrations, so they may be reapplied on load. Despite storing additional parameters these files are far smaller than comparable '.csv' text-images and maintain accessibility by only requiring the NumPy library for access.

CONCLUSION

Pew^2 is the first open-source, multiple-vendor compatible, imaging and analysis software specifically designed for LA-ICP-MS research. It was written with several design philosophies to minimise data bias, maximise analytical rigour and allow verification by third parties. The open nature of the program assists in ensuring its longevity and adoption. Features included in this software follow fast and simple workflows for the production of publication-ready, quantified, and processed images from raw instrument data.

ASSOCIATED CONTENT

Supporting Information

Supporting figures and links (DOCX)
Raw data (ZIP)

AUTHOR INFORMATION

Corresponding Author

* Philip A. Doble, philip.doble@uts.edu.au.

Present Addresses

†If an author's address is different than the one given in the affiliation line, this information may be included here.

Author Contributions

TEL performed all data acquisition and software design. The manuscript was written through contributions of all authors.

REFERENCES

(1)   Gray, A. L. Solid Sample Introduction by Laser Ablation for Inductively Coupled Plasma Source Mass Spectrometry. *Analyst* **1985**, *110* (5), 551–556. https://doi.org/10.1039/AN9851000551.

(2)   Hare, D. J.; Shimoni, O.; Bishop, D. P. The Immuno-Mass Spectrometry Chemical Microscope. *Trends Chem.* **2020**, *2* (5), 403–406. https://doi.org/10.1016/j.trechm.2020.02.014.

(3)   Pozebon, D.; Scheffler, G. L.; Dressler, V. L.; Nunes, M. A. G. Review of the Applications of Laser Ablation Inductively Coupled Plasma Mass Spectrometry (LA-ICP-MS) to the Analysis of Biological Samples. *J. Anal. At. Spectrom.* **2014**, *29* (12), 2204–2228. https://doi.org/10.1039/C4JA00250D.

(4)   Limbeck, A.; Galler, P.; Bonta, M.; Bauer, G.; Nischkauer, W.; Vanhaecke, F. Recent Advances in Quantitative LA-ICP-MS Analysis: Challenges and Solutions in the Life Sciences and Environmental Chemistry. *Anal. Bioanal. Chem.* **2015**, *407* (22), 6593–6617. https://doi.org/10.1007/s00216-015-8858-0.

(5)   Chew, D.; Drost, K.; Marsh, J. H.; Petrus, J. A. LA-ICP-MS Imaging in the Geosciences and Its Applications to Geochronology. *Chem. Geol.* **2021**, *559*, 119917. https://doi.org/10.1016/j.chemgeo.2020.119917.

(6)   Li, X.; Liu, T.; Chang, C.; Lei, Y.; Mao, X. Analytical Methodologies for Agrometallomics: A Critical Review. *J. Agric. Food Chem.* **2021**, *69* (22), 6100–6118. https://doi.org/10.1021/acs.jafc.1c00275.

(7)   Weiskirchen, R.; Weiskirchen, S.; Kim, P.; Winkler, R. Software Solutions for Evaluation and Visualization of Laser Ablation Inductively Coupled Plasma Mass Spectrometry Imaging (LA-ICP-MSI) Data: A Short Overview. *J. Cheminform.* **2019**, *11* (1). https://doi.org/10.1186/s13321-019-0338-7.

(8)   López-Fernández, H.; De S Pessôa, G.; Arruda, M. A. Z.; Capelo-Martínez, J. L.; Fdez-Riverola, F.; Glez-Peña, D.; Reboiro-Jato, M. LA-IMageS: A Software for Elemental Distribution Bioimaging Using LA-ICP-MS Data. *J. Cheminform.* **2016**, *8* (1), 1–10. https://doi.org/10.1186/s13321-016-0178-7.

(9)   Van Malderen, S.; Vincze, L.; Vanhaecke, F. HDIP : Powerful LA-ICP-MS Data Reduction Software with Extensive Data Interogation Tools. In *NAWLA19, North American Workshop on Laser Ablation 2019, Abstracts*; 2019; p 23.

(10)   Suzuki, T.; Sakata, S.; Makino, Y.; Obayashi, H.; Ohara, S.; Hattori, K.; Hirata, T. IQuant2: Software for Rapid and Quantitative Imaging Using Laser Ablation-ICP Mass Spectrometry. *Mass Spectrom.* **2018**, *7* (1), A0065–A0065. https://doi.org/10.5702/massspectrometry.a0065.

(11)   Uerlings, R.; Matusch, A.; Weiskirchen, R. Reconstruction of Laser Ablation Inductively Coupled Plasma Mass Spectrometry (LA-ICP-MS) Spatial Distribution Images in Microsoft Excel 2007. *Int. J. Mass Spectrom.* **2016**, *395*, 27–35. https://doi.org/10.1016/j.ijms.2015.11.010.

(12)   Osterholt, T.; Salber, D.; Matusch, A.; Becker, J. S.; Palm, C. IMAGENA: Image Generation and Analysis - An Interactive Software Tool Handling LA-ICP-MS Data. *Int. J. Mass Spectrom.* **2011**, *307* (1–3), 232–239. https://doi.org/10.1016/j.ijms.2011.03.010.

(13)   Managh, A. J.; Reid, P. A New Freeware Tool for Image Processing and Its Application to High Speed LA-ICP-MS Imaging. *J. Anal. At. Spectrom.* **2019**, *34* (7), 1369–1373. https://doi.org/10.1039/c9ja00082h.

(14)   Paton, C.; Hellstrom, J.; Paul, B.; Woodhead, J.; Hergt, J. Iolite: Freeware for the Visualisation and Processing of Mass Spectrometric Data. *J. Anal. At. Spectrom.* **2011**, *26* (12), 2508. https://doi.org/10.1039/c1ja10172b.

(15)   Sforna, M. C.; Lugli, F. MapIT!: A Simple and User-Friendly MATLAB Script to Elaborate Elemental Distribution Images from LA-ICP-MS Data. *J. Anal. At. Spectrom.* **2017**, *32* (5), 1035–1043. https://doi.org/10.1039/C7JA00023E.

(16)   Castellanos-García, L. J.; Gokhan Elci, S.; Vachet, R. W. Reconstruction, Analysis, and Segmentation of LA-ICP-MS Imaging Data Using Python for the Identification of Sub-Organ Regions in Tissues. *Analyst* **2020**, *145* (10), 3705–3712. https://doi.org/10.1039/C9AN02472G.

(17)   Bianga, J.; Bouslimani, A.; Bec, N.; Quenet, F.; Mounicou, S.; Szpunar, J.; Bouyssiere, B.; Lobinski, R.; Larroque, C. Complementarity of MALDI and LA ICP Mass Spectrometry for Platinum Anticancer Imaging in Human Tumor. *Metallomics* **2014**, *6* (8), 1382–1386. https://doi.org/10.1039/C4MT00131A.

(18)   Gundlach-Graham, A.; Günther, D. Toward Faster and Higher Resolution LA–ICPMS Imaging: On the Co-Evolution of LA Cell Design and ICPMS Instrumentation. *Anal. Bioanal. Chem.* **2016**, *408* (11), 2687–2695. https://doi.org/10.1007/s00216-015-9251-8.

(19)   Schindelin, J.; Arganda-Carreras, I.; Frise, E.; Kaynig, V.; Longair, M.; Pietzsch, T.; Preibisch, S.; Rueden, C.; Saalfeld, S.; Schmid, B.; Tinevez, J.-Y.; White, D. J.; Hartenstein, V.; Eliceiri, K.; Tomancak, P.; Cardona, A. Fiji: An Open-Source Platform for Biological-Image Analysis. *Nat. Methods* **2012**, *9* (7), 676–682. https://doi.org/10.1038/nmeth.2019.

(20)   Chen, X.; Dallmeier-Tiessen, S.; Dasler, R.; Feger, S.; Fokianos, P.; Gonzalez, J. B.; Hirvonsalo, H.; Kousidis, D.; Lavasa, A.; Mele, S.; Rodriguez, D. R.; Šimko, T.; Smith, T.; Trisovic, A.; Trzcinska, A.; Tsanaktsidis, I.; Zimmermann, M.; Cranmer, K.; Heinrich, L.; Watts, G.; Hildreth, M.; Lloret Iglesias, L.; Lassila-Perini, K.; Neubert, S. Open Is Not Enough. *Nat. Phys.* **2019**, *15* (2), 113–119. https://doi.org/10.1038/s41567-018-0342-2.

(21)   Alomari, H. W.; Ramasamy, V.; Kiper, J. D.; Potvin, G. A User Interface (UI) and User EXperience (UX) Evaluation Framework for Cyberlearning Environments in Computer Science and Software Engineering Education. *Heliyon* **2020**, *6* (5), e03917. https://doi.org/10.1016/j.heliyon.2020.e03917.

(22)   O'Donoghue, S. I.; Baldi, B. F.; Clark, S. J.; Darling, A. E.; Hogan, J. M.; Kaur, S.; Maier-Hein, L.; McCarthy, D. J.; Moore, W. J.; Stenau, E.; Swedlow, J. R.; Vuong, J.; Procter, J. B. Visualization of Biomedical Data. *Annu. Rev. Biomed. Data Sci.* **2018**, *1* (1), 275–304. https://doi.org/10.1146/annurev-biodatasci-080917-013424.

(23)   Borland, D.; Taylor, R. M. Rainbow Color Map (Still) Considered Harmful. *IEEE Comput. Graph. Appl.* **2007**, *27* (2), 14–17. https://doi.org/10.1109/MCG.2007.323435.

(24)   Borkin, M.; Gajos, K.; Peters, A.; Mitsouras, D.; Melchionna, S.; Rybicki, F.; Feldman, C.; Pfister, H. Evaluation of Artery Visualizations for Heart Disease Diagnosis. *IEEE Trans. Vis. Comput. Graph.* **2011**, *17* (12), 2479–2488. https://doi.org/10.1109/TVCG.2011.192.

(25)   Paul, B.; Hare, D. J.; Bishop, D. P.; Paton, C.; Nguyen, V. T.; Cole, N.; Niedwiecki, M. M.; Andreozzi, E.; Vais, A.; Billings, J. L.; Bray, L.; Bush, A. I.; McColl, G.; Roberts, B. R.; Adlard, P. A.; Finkelstein, D. I.; Hellstrom, J.; Hergt, J. M.; Woodhead, J. D.; Doble, P. A. Visualising Mouse Neuroanatomy and Function by Metal Distribution Using Laser Ablation-Inductively Coupled Plasma-Mass Spectrometry Imaging. *Chem. Sci.* **2015**, *6* (10), 5383–5393. https://doi.org/10.1039/C5SC02231B.

(26)   Hare, D.; Burger, F.; Austin, C.; Fryer, F.; Grimm, R.; Reedy, B.; Scolyer, R. A.; Thompson, J. F.; Doble, P. Elemental Bio-Imaging of Melanoma in Lymph Node Biopsies. *Analyst* **2009**, *134* (3), 450–453. https://doi.org/10.1039/B812745J.

(27)   Aonishi, T.; Hirata, T.; Kuwatani, T.; Fujimoto, M.; Chang, Q.; Kimura, J.-I. A Numerical Inversion Method for Improving the Spatial Resolution of Elemental Imaging by Laser Ablation-Inductively Coupled Plasma-Mass Spectrometry. *J. Anal. At. Spectrom.* **2018**, *33* (12), 2210–2218. https://doi.org/10.1039/C7JA00334J.

(28)   Van Malderen, S. J. M.; van Elteren, J. T.; Vanhaecke, F. Development of a Fast Laser Ablation-Inductively Coupled Plasma-Mass Spectrometry Cell for Sub-Mm Scanning of Layered Materials. *J. Anal. At. Spectrom.* **2015**, *30* (1), 119–125. https://doi.org/10.1039/C4JA00137K.

(29)   Harris, C. R.; Millman, K. J.; van der Walt, S. J.; Gommers, R.; Virtanen, P.; Cournapeau, D.; Wieser, E.; Taylor, J.; Berg, S.; Smith, N. J.; Kern, R.; Picus, M.; Hoyer, S.; van Kerkwijk, M. H.; Brett, M.; Haldane, A.; del Río, J. F.; Wiebe, M.; Peterson, P.; Gérard-Marchant, P.; Sheppard, K.; Reddy, T.; Weckesser, W.; Abbasi, H.; Gohlke, C.; Oliphant, T. E. Array Programming with NumPy. *Nature* **2020**, *585* (7825), 357–362. https://doi.org/10.1038/s41586-020-2649-2.

(30)   Westerhausen, M. T.; Lockwood, T. E.; Gonzalez de Vega, R.; Röhnelt, A.; Bishop, D. P.; Cole, N.; Doble, P. A.; Clases, D. Low Background Mould-Prepared Gelatine Standards for Reproducible Quantification in Elemental Bio-Imaging. *Analyst* **2019**, *144* (23), 6881–6888. https://doi.org/10.1039/c9an01580a.

(31)   Wee, A.; Grayden, D. B.; Zhu, Y.; Petkovic-Duran, K.; Smith, D. A Continuous Wavelet Transform Algorithm for Peak Detection. *Electrophoresis* **2008**, *29* (20), 4215–4225. https://doi.org/10.1002/elps.200800096.

(32)   Almeida, A. M.; Castel-Branco, M. M.; Falcão, A. C. Linear Regression for Calibration Lines Revisited: Weighting Schemes for Bioanalytical Methods. *J. Chromatogr. B Anal. Technol. Biomed. Life Sci.* **2002**, *774* (2), 215–222. https://doi.org/10.1016/S1570-0232(02)00244-1.

(33)   Costes, S. V.; Daelemans, D.; Cho, E. H.; Dobbin, Z.; Pavlakis, G.; Lockett, S. Automatic and Quantitative Measurement of Protein-Protein Colocalization in Live Cells. *Biophys. J.* **2004**, *86* (6), 3993–4003. https://doi.org/10.1529/biophysj.103.038422.

(34)   Eliceiri, K. W.; Berthold, M. R.; Goldberg, I. G.; Ibáñez, L.; Manjunath, B. S.; Martone, M. E.; Murphy, R. F.; Peng, H.; Plant, A. L.; Roysam, B.; Stuurmann, N.; Swedlow, J. R.; Tomancak, P.; Carpenter, A. E. Biological Imaging Software Tools. *Nat. Methods* **2012**, *9* (7), 697–710. https://doi.org/10.1038/nmeth.2084.